DOI: 10.13009/EUCASS2023-057
Aerospace Europe Conference 2023 – 10TH EUCASS – 9TH CEAS

A Dual-Based Linear Programming Formulation of Optimal Control: Fuel-Optimal Rendezvous Guidance and Boresight Pointing Applications

Sergio Cuevas del Valle⋆†*, Pablo Solano-López*⋆ *and Hodei Urrutxua*⋆
⋆*Aerospace Systems and Transport Research Group, Universidad Rey Juan Carlos*
Camino del Molino 5, 28942, Fuenlabrada, Spain
s.cuevas.2017@alumnos.urjc.es · pablo.solano@urjc.es · hodei.urrtxua@urjc.es
†Corresponding author

Abstract

This work develops a new cost-efficient solver to formulate fuel-optimal control problems: in particular, Alternating Direction Method of Multipliers and Model Predictive Control are used to close the gap between L_1 and L_2 optimization in classical astrodynamics problems. The combination of these two algorithms allows to render general NLP fuel-optimal problems solvable by Linear Programming techniques independently of the fuel-consumption proxy used. Moreover, their low footprint makes them a solid candidate for real-time, embedded applications. These novel techniques are applied to several rendezvous and orbital transfer test cases in both the Keplerian and the Circular Restricted Three-Body Problems, together with impulsive attitude slews.

1. Introduction

Optimal control problems are ubiquitous within astrodynamics and general mission design of aerospace vehicles, in which tight performance constraints exist. Along this line, fuel-optimal performance is of vital interest, as carrying additional fuel is contrary to payload capacity. The design of fuel-optimal state trajectories is a major challenge is space dynamics for which no closed solution can a-priori be found.

Despite the vast literature and effort on the topic, Optimal Control Theory is still an open line of research just leaving its infancy, especially with regards to Real Time Optimal Control onboard legacy systems. The design of optimal control laws is constrained by the need to solve complex nonlinear programming problems (NLP) associated to a Hamiltonian Minimization Condition, either in the form of Pontryagin's Maximum Principle or the complementary Hamilton-Jacobi-Bellman PDE equation.[1] The reduction of such computational burden is always a desirable goal and is actually the main focus of this work.

Fuel optimal problems are a prominent problematic in space dynamics optimization since the very times of the foundation of modern Optimal Control Theory and the celebrated question by Edelbaum.[2] In fact, in the late 1960s, Primer Vector Theory (PVT) was born, as the result of the application of Pontryagin's Maximum Principle to the problem of impulsive space trajectory optimization. In this sense, the seminar work of Lawden, Neudstadt, Potter, Prussing et al.[3–6] remains as a solid foundation for the latest developments in the field,[7,8] although numerical techniques are now predominant over analytical studies. In this sense, convex optimization and Model Predictive Control (MPC) are becoming standard technologies for general optimal control.[9] Recent advances have led to the introduction of alternative solving strategies within space dynamics convex optimization, such as Alternating Direction Method of Multipliers (ADMM), as shown in Le Cleac'h and Manchester;[10] which also already shows relevant applications in combination with MPC schemes.[11,12]

Compared to previous literature, this communication presents novel formulations of general constrained fuel-optimal control problem through modern optimization techniques, mainly ADMM and MPC, founded on classical PVT results. These techniques allow to establish a cost mapping principle between fuel-optimal and quadratic-cost problems; moreover, compared to previous works, the latter are solved exploiting their dual-problem formulation, for which a simple close-form solution exists in the form of a root-finding problem. Under this new paradigm, general NLP fuel-optimal problems are rendered solvable by Linear Programming, inexpensive techniques. The low footprint of the proposed algorithms makes them a solid candidate for real-time, embedded applications, providing optimal solutions

DOI: 10.13009/EUCASS2023-057

at nearly null expenses. The proposed solvers are applied to several rendezvous missions to objectively assess their performance. Additionally, the same methodology is applied to the design of rest-to-rest attitude slews.

The remainder of this paper is organized as follows. Section 2 introduces an abstract formulation of the general optimal constrained linear regulation problem, with remarks to general in-orbit rendezvous and attitude control. Some classical results on Primer Vector Theory are presented in Section 4, on which further developments presented in this work are built, together with their intrinsic analytical and computational problematics. The mathematical algorithms exploited in the proposed solutions are detailed in Section 5, where some fundamentals in the Theory of Proximal Operators and Alternating Direction Method of Multipliers are discussed. Sections 6 and 7 details the numerical and computational, close-form recursive solutions proposed to solve the original regulation problems, while Section 9 provides several real-case mission scenarios to validate and verify their performance and design. Finally, open lines of research and key takeaways are summarized in Section 10.

2. Optimal Linear Impulsive Regulation in Space Dynamics

This Section introduces the problems of interest to be solved in this paper: given their relevance in space dynamics, optimal impulsive regulation of general dynamical systems will be the focus of our study.

2.1 The General Regulation Bolza Problem

In fact, the objective of this paper is to propose novel algorithmic solutions to realizations of the following affine optimal control problem

$$
\begin{aligned}
\underset{\mathbf{u}\in\mathbb{U}}{\arg\min} \quad & J = G\left(\mathbf{s}(t_f), \mathbf{s}(0), t_f, t_0\right) + \int_{t_0}^{t_f} l\left(\mathbf{s}, \mathbf{u}, t\right) \mathrm{d}t \\
\text{subject to} \quad & \dot{\mathbf{s}} = \mathbf{f}(\boldsymbol{\mu}, \mathbf{s}) + B(t)\,\mathbf{u}\ , \\
& \mathbf{s}(t_0) = \mathbf{s}_0\ , \\
& \mathbf{s}(t_f) = \mathbf{0}\ , \\
& \mathbf{g}(\boldsymbol{\mu}, \mathbf{s}) = \mathbf{0}\ , \\
& \mathbf{h}(\boldsymbol{\mu}, \mathbf{s}) < \mathbf{0}\ , \\
& u_{\min} \leq ||\mathbf{u}||_p \leq u_{\max}\ ,
\end{aligned}
\tag{1}
$$

where the state of the dynamical system is described by the vector $\mathbf{s}$ and whose first-order evolution with respect to the independent variable t is governed by the vector field $\mathbf{f}$, characterized by a set of parameters $\boldsymbol{\mu}$ and the control vector field $\mathbf{u}$.

The solution is given by the determination of the phase space flow $\mathbf{s}^*(t)$ and control application $\mathbf{u}^*(t)$ minimizing the cost function J while satisfying the boundary conditions equalities $\mathbf{g}$ and path constraints $\mathbf{h}$. In the latter case, $||\mathbf{u}||_p$ denotes the p-norm of the control action $\mathbf{u}$, which can be used to promote either control sparsity, or to model actuation saturation and control authority penalties.

The differential equations for the state dynamics can be however expressed in a more convenient way for our purpose. Indeed, in the design of guidance and control schemes, the following form of the state flow, as given by Lagrange's formula, is usually leveraged

$$
\mathbf{s}(t) = \Phi(t, t_0)\,\mathbf{s}_0 + \int_{t_0}^{t} \Phi(t-\tau, \tau)\,B\,\mathbf{u}(\tau)\,\mathrm{d}\tau\ .
$$

The first term corresponds to the homogeneous solution of the dynamics, given by the discrete mapping of the initial conditions to the epoch of interest t through the State Transition Matrix (STM) of the system Φ. The convolutional, integral term constitutes the effect of the control action $\mathbf{u}(t)$ through the control input matrix B on the dynamics.

In astrodynamics applications, a discrete or impulsive manoeuvre sequence is usually conceived as a feasible and natural control strategy. Particularising Lagrange's formula for such action plan $\mathbf{u}(t) = \sum_i \mathbf{U}_i\,\delta(t-t_i)$ yields the following result

$$
\mathbf{s}(t) = \Phi(t, t_0)\,\mathbf{s}_0 + \sum_{i=1}^{N} \Phi(t, t_i)\,B\,\mathbf{U}_i
\tag{2}
$$

DOI: 10.13009/EUCASS2023-057

where the $\delta(t - t_i)$ is Dirac's delta generalized function. Introducing the time shifting property of the STM, the above result can be further expanded as

$$\mathbf{s}(t) = \Phi(t, t_0)\, \mathbf{s}_0 + \sum_{i=1}^{N} \Phi(t, t_0)\, \Phi(t_i, t_0)^{-1} B\, \mathbf{U}_i \ .$$

Some guidance techniques, such as those presented in here, are founded on the premise of discrete dynamics. The classical results just presented can be used to construct a discrete map $\mathbf{s}(t_{i+1}) = \mathbf{F}(\mathbf{s}(t_i))$ for a given discrete time sequence 0, t_i, t_{i+1}..., under the action of both continuous and discrete control functions. For the latter case,

$$\mathbf{s}_{i+1} = \Phi(t_{i+1}, t_0)\, \Phi(t_i, t_0)^{-1}\, \mathbf{s}_i + \Phi(t_{i+1}, t_0)\, \Phi(t_i, t_0)^{-1} B\, \mathbf{U}_i \ .$$

Finally, depending on the system dynamics $\mathbf{f}$ and the status of the final time as a decision variable or as a fixed parameter, four different regulation problems can be identified, as compiled in Table 1.

	Time-fixed	Time-free
Linear	Type A	Type C
Nonlinear	Type B	Type D

Table 1: Regulation problems of interest.

This preliminary study proposes a novel close-form, low-footprint, fast and accurate solver for Types A and B (time-fixed). Solutions to Types C and D are currently under development and remain as an open line of research.

3. The time-fixed, L_p Regulation Problem

In space dynamics, minimization of fuel consumption is a primary goal in impulsive trajectory planning (energy investment applies for continuous actions). Therefore, the running cost l_i is further particularised to represent a control effort metric or performance index, given by the integral l_p-norm of the control action sequence $\mathbf{U}_i$. Moreover, the final end cost G may be dropped without loss of generality, so that finally, after discretization of the dynamics, the general Bolza problem in Eqs. (1) is transcribed into the following equivalent form

$$\begin{aligned}
\underset{\mathbf{U}_i}{\arg\min} \quad & J = \sum_i \|\mathbf{U}_i\|_p \\
\text{subject to} \quad & \mathbf{s}_f - \Phi(t_f, t_0)\, \mathbf{s}_0 = \sum_i \Phi(t_f, t_i)\, B(t_i)\, U_i \ , \\
& \mathbf{s}(t_0) = \mathbf{s}_0 \ , \\
& \mathbf{s}(t_f) = \mathbf{0} \ , \\
& \mathbf{g}(\boldsymbol{\mu}, \mathbf{s}) = \mathbf{0} \ , \\
& \mathbf{h}(\boldsymbol{\mu}, \mathbf{s}) < \mathbf{0} \ , \\
& u_{\min} \leq \|\mathbf{U}_i\|_p \leq u_{\max} \ ,
\end{aligned}$$

Different p-norms provide different proxies to fuel consumption. In fact, it can be shown that only the l_2, l_1 and l_∞ norms (globally referred to as L_1 metrics) have physical significance when dealing with impulsive thrusting units,[13] despite the common use of the squared l_2-norm, denoted l_2^2. These are defined as, for a vector $\mathbf{v} \in \mathbb{R}^n$,

$$\|\mathbf{v}\|_2 = \sqrt{\mathbf{v}^\intercal\, \mathbf{v}}\,, \quad \|\mathbf{v}\|_1 = \sum_{i=1}^{n} |v_i|\,, \quad \|\mathbf{v}\|_\infty = \max |v_i|\,.$$

Quadratic penalties L_2, such as the l_2^2, provide however analytical solutions to these optimal problems (see the Linear Quadratic Gaussian), and therefore are the workhorse in Aerospace Engineering when it comes to trajectory optimization and planning. The following Sections explore numerical techniques to close the gap between L_1 and L_2 optimization in terms of finding close-form solutions for the former.

3.1 Dynamics of interest

Section 9 provides simulation examples in which the proposed algorithms are verified and validated via objective analysis of their performance. The dynamics of these systems of interest are now briefly described.

DOI: 10.13009/EUCASS2023-057

Keplerian Rendezvous Orbital rendezvous may be basically defined as making a spacecraft, named the chaser, acquire the same position and velocity as a given reference, known as the target, which may be a physical or virtual object.

Let the target's centre of mass position be described by the vector $\mathbf{r}_t$. Introducing the Euler-Hill reference frame, composed of the the R-bar $\mathbf{u}_r$, V-bar $\mathbf{u}_v$ and H-bar $\mathbf{u}_h$ directions, by definition,

$$\mathbf{r}_t = r_t\,\mathbf{u}_r, \quad \mathbf{u}_h = \frac{\mathbf{h}}{h}, \quad \mathbf{u}_v = \mathbf{u}_h \times \mathbf{u}_r\,. \tag{3}$$

In this case, $\mathbf{h}$ is the specific angular momentum of the target. In the same fashion, let the chaser's center of mass be described by $\mathbf{r}_c$. The relative position vector $\boldsymbol{\rho}$ is now defined as

$$\boldsymbol{\rho} = \mathbf{r}_c - \mathbf{r}_t = x\,\mathbf{u}_r + y\,\mathbf{u}_v + z\,\mathbf{u}_h \tag{4}$$

In an inertial frame, differentiating twice Eq. (4) with respect to time and incorporating the appropriate Newtonian gravity field term yields

$$\ddot{\boldsymbol{\rho}} = \frac{\mu}{r_t^3}\mathbf{r}_t - \frac{\mu}{\|\mathbf{r}_t + \boldsymbol{\rho}\|^3}(\mathbf{r}_t + \boldsymbol{\rho})$$

where μ is the gravitational parameter of the primary or massive body in consideration. Realizing the previous vector equation in the Euler-Hill frame, which is non-inertial, the following result arises

$$\ddot{\boldsymbol{\rho}} + 2\boldsymbol{\omega}\times\dot{\boldsymbol{\rho}} + \dot{\boldsymbol{\omega}}\times\boldsymbol{\rho} + \boldsymbol{\omega}\times\boldsymbol{\omega}\times\boldsymbol{\rho} = \frac{\mu}{r_t^3}\mathbf{r}_t - \frac{\mu}{\|\mathbf{r}_t + \boldsymbol{\rho}\|^3}(\mathbf{r}_t + \boldsymbol{\rho}) \tag{5}$$

where $\boldsymbol{\omega} = \omega\,\mathbf{u}_h$ and $\dot{\boldsymbol{\omega}} = \dot{\omega}\,\mathbf{u}_h$ are the angular velocity and acceleration, respectively, of the Euler-Hill frame with respect to the inertial frame, but realized in the former.

However, rendezvous applications in the Keplerian, two-body regime are usually rather founded on linear relative motion models, among which the Hill-Clohessy-Wiltshire (HCW) system is one of the most common choices. Although Hill arrived at the very same result when studying the Moon's motion as seen from the Earth nearly a century before,[14] this set of equations were again developed and popularized in the 1960s to study Keplerian rendezvous missions.[15] This linear model arises when the gravitational terms of the complete relative motion nonlinear equations are expressed in Taylor series, assuming a circular target's orbit, with $\dot{\omega} = 0$ and $\omega = n = \mu^{1/2}\,r_t^{-3/2}$ and the assumption of a close range relative state $\rho/r_t \ll 1$, so that Hill-Clohessy-Wiltshire equations are of the form[15]

$$\begin{aligned} \ddot{x} - 2n\dot{y} - 3n^2x &= 0\,, \\ \ddot{y} + 2n\dot{x} &= 0\,, \\ \ddot{z} + n^2 z &= 0\,. \end{aligned} \tag{6}$$

Their non-homogeneous form may take into account any other orbital perturbation or control actions. To our advantage, the STM of the HCW model is analytical. However, if the circular orbit assumption is relaxed, the equivalence between time and true anomaly as the independent variable of the equations of motion breaks,[3,16] giving rise to different State Transition Matrices.[17–20]

CR3BP Rendezvous A similar result to the nonlinear Keplerian system Eqs. (5) can be actually derived for the CR3BP, in which the target and chaser are not only influenced by the gravitational well of a massive body, but by two of them, known as the primaries, and whose relative state is described by a planar circular Keplerian orbit.

When realised in the natural synodic reference frame to the primaries' motion, the relative state between the target and the chaser is described by the following set of nonlinear equations[21,22]

$$\begin{aligned} \mathbf{r}_t &= \begin{bmatrix}\xi & \chi & \eta\end{bmatrix}^\intercal\,, \\ \ddot{x} - 2\dot{y} - x &= (1-\mu)\left(\frac{\xi+\mu}{\|\mathbf{r}_t - \mathbf{R}_1\|^3} - \frac{x+\xi+\mu}{\|\boldsymbol{\rho}+\mathbf{r}_t - \mathbf{R}_1\|^3}\right) + \mu\left(\frac{\xi-1+\mu}{\|\mathbf{r}_t - \mathbf{R}_2\|^3} - \frac{x+\xi-1+\mu}{\|\boldsymbol{\rho}+\mathbf{r}_t - \mathbf{R}_2\|^3}\right) + u_x, \\ \ddot{y} + 2\dot{x} - y &= (1-\mu)\left(\frac{\eta}{\|\mathbf{r}_t - \mathbf{R}_1\|^3} - \frac{y+\eta}{\|\boldsymbol{\rho}+\mathbf{r}_t - \mathbf{R}_1\|^3}\right) + \mu\left(\frac{\eta}{\|\mathbf{r}_t - \mathbf{R}_2\|^3} - \frac{y+\eta}{\|\boldsymbol{\rho}+\mathbf{r}_t - \mathbf{R}_2\|^3}\right) + u_y, \\ \ddot{z} &= (1-\mu)\left(\frac{\zeta}{\|\mathbf{r}_t - \mathbf{R}_1\|^3} - \frac{z+\zeta}{\|\boldsymbol{\rho}+\mathbf{r}_t - \mathbf{R}_1\|^3}\right) + \mu\left(\frac{\zeta}{\|\mathbf{r}_t - \mathbf{R}_2\|^3} - \frac{z+\zeta}{\|\boldsymbol{\rho}+\mathbf{r}_t - \mathbf{R}_2\|^3}\right) + u_z. \end{aligned} \tag{7}$$

In the above result, μ is the normalised gravitational parameter of the orbit $M_2/(M_1 + M_2)$, where M_i is the mass of the primaries. Moreover, it is customary to use dimensionless coordinates, such that the distance between

DOI: 10.13009/EUCASS2023-057

the primaries is used as characteristic length and their orbital period around their common barycenter is taken as characteristic time. In these dimensionless coordinates, the primaries revolve at one radian per unit of dimensionless time and show constant position vectors

$$\mathbf{R}_1 = -\mu\,\mathbf{i}\,, \quad \mathbf{R}_2 = (1-\mu)\,\mathbf{i}\,.$$

Retaining up to first order terms in Eqs. (7) yields the Rendezvous Linear Model (RLM),[22,23] which can be compactly expressed in matrix form as:

$$\dot{\mathbf{s}} = A\mathbf{s} + B\mathbf{u} = \begin{bmatrix}\dot{\boldsymbol{\rho}}\\ \ddot{\boldsymbol{\rho}}\end{bmatrix} = \begin{pmatrix}0_{3\times3} & I_{3\times3}\\ \Sigma & \Omega\end{pmatrix}\begin{bmatrix}\boldsymbol{\rho}\\ \dot{\boldsymbol{\rho}}\end{bmatrix} + \begin{pmatrix}0_{3\times3}\\ I_{3\times3}\end{pmatrix}\mathbf{u}, \tag{8}$$

where $0_{3\times3}$ and $I_{3\times3}$ denotes 3-dimensional null and identity matrices, respectively; the Coriolis acceleration term Ω reads

$$\Omega = \begin{pmatrix}0 & 2 & 0\\ -2 & 0 & 0\\ 0 & 0 & 0\end{pmatrix}$$

and the Hessian matrix Σ can be computed as

$$\Sigma = -(\kappa_1+\kappa_2)\,I_{3\times3} + 3\,\kappa_1\,(\mathbf{e}_1\otimes\mathbf{e}_1) + 3\,\kappa_2\,(\mathbf{e}_2\otimes\mathbf{e}_2),$$

where the operator $\otimes$ denotes the dyadic product, $\mathbf{e}_i$ are unit vectors pointing from the i-th primary to the target spacecraft and the κ_i are coefficients defined as

$$\mathbf{e}_i = \frac{\mathbf{r}_\mathrm{t}-\mathbf{R}_i}{\|\mathbf{r}_\mathrm{t}-\mathbf{R}_i\|}\,, \quad \kappa_i = \frac{\mu_i}{\|\mathbf{r}_\mathrm{t}-\mathbf{R}_i\|^3}. \qquad i = 1,2\,.$$

While the original RLM model was derived as a linearization of the true relative dynamics around the target position vector, in this work we exploit the Relative Libration Linear Model (RLLM), which considers relative motion near the collinear libration points, assuming both the target and chaser spacecraft to be on an LPO. In such cases, Σ is expected to become constant or (quasi-)periodic, respectively and can be shown to read[22]

$$\Sigma = \begin{pmatrix}1+2c_2 & 0 & 0\\ 0 & 1-c_2 & 0\\ 0 & 0 & -c_2\end{pmatrix}.$$

The fundamental frequency c_2 depends on the libration point both spacecraft orbit, as defined in Richardson.[24]

Attitude slews Additionally, boresight pointing applications or general attitude slews are also studied under the light of impulsive torques, such as those provided by Reaction Control Systems (RCS).

The attitude dynamics are described by the following Initial Value Problem (IVP), composed of Euler's equations of the rigid body with appropriate initial conditions

$$I\dot{\omega} + \omega\times I\omega = \mathbf{u}\,, \qquad \omega\,(0) = \omega_0\,. \tag{9}$$

The angular velocity $\boldsymbol{\omega}$ shall be realised in the body frame of the system, in which the inertia dyadic I is constant in time.

The kinematics of the problem are expressed through Shuster's unit quaternions $\mathbf{q} = [\mathbf{q}_v,\, q_4]^\intercal = [\sin\theta/2\,\mathbf{e},\, \cos\theta/2]^\intercal$, which describe rotations from the global, departure reference frame to the objective, local one (contrary to those of Hamilton, which provides the inverse transformation).[25] The IVP describing the quaternion evolution in time is

$$\dot{\mathbf{q}} = \frac{1}{2}\omega\otimes\mathbf{q}\,, \qquad \mathbf{q}(0) = \mathbf{q}_0\,. \tag{10}$$

The $\otimes$ operator here describes the quaternion product, given by the following $SO(4)$ isoclinic rotation Q

$$\mathbf{q}_1\otimes\mathbf{q}_2 = Q(\mathbf{q}_1)\,\mathbf{q}_2 = \begin{pmatrix}q_4 I - \hat{\mathbf{q}}_v & \mathbf{q}_v\\ -\mathbf{q}_v^\intercal & q_4\end{pmatrix}\mathbf{q}_2\,,$$

for which the *hat map* $\wedge : \mathbb{R}^3 \to \mathfrak{so}(3)$, an isometry between $\mathbb{R}^3$ and $\mathfrak{so}(3)$, is defined such that $\hat{\mathbf{x}} = -\mathbf{x}^\intercal$ and $\hat{\mathbf{x}}\mathbf{y} = \mathbf{x}\times\mathbf{y}$. Moreover, in the above results, the angular velocity is overloaded to be a pure quaternion, $\boldsymbol{\omega} \to [\boldsymbol{\omega}, 0]^\intercal$.

Discrete transitions for the attitude problem are available via the STM matrix of the problem.

DOI: 10.13009/EUCASS2023-057

4. Analytical solutions

Classical optimal impulsive control theory for linear systems is developed in this Section, mainly applied to classical orbit transfers in space dynamics. These results suppose the foundation of the developments to follow.

4.1 Classical Primer Vector Theory

In the late 1960s, the foundational works of Lawden et al.[3,6,26,27] in space trajectory optimization for impulsive probes led to the seminar Primer Vector Theory,[28] which establishes the necessary and sufficient conditions for optimal transport within Newtonian gravity. These arises as the result of the application of Pontryagin's Maximum Principle to the problem of optimal impulsive control.

These necessary conditions (NCS) are conveniently expressed via the adjoint of the velocity vector $\boldsymbol{\lambda}_v$, named the primer vector by Lawden or $\mathbf{p}$.

$$\mathbf{p} = -\boldsymbol{\lambda}_v \,.$$

In practice, these NCS may be used, for example, to determine optimal additional mid-course impulses to a given planned sequence to reduce fuel consumption. The modern formal statement of the necessary and sufficient conditions is due to Carter,[29] although his augmented system of 8 constraints is fundamentally equivalent to those presented here and is therefore omitted for brevity. Informally, they read[28]

1. The primer vector and its first derivative are continuous everywhere.
2. The Euclidean norm of the primer vector satisfies $p(t) \leq 1$ with the impulses occurring at those instants at which $p(t) = 1$.
3. At the impulse times the primer vector is a unit vector in the optimal thrust direction.
4. As a consequence of the above conditions, $\dot{\mathbf{p}}^\intercal \mathbf{p} = 0$ at an intermediate impulse (not at the initial or final time).

4.2 Neustadt-Potter Theorem: Maximum Number of Impulses

A fundamental result to this communication is the Maximum Number of Impulses Theorem by Neustadt and Potter,[4,5,30] which has a long tradition within rendezvous studies since the times of Edelbaum.[2,8]

Informally, it states that for a time-fixed linear system of dimension q, the regulation solution requires at most q impulses and such solution is also optimal.

Based on this result, Potter cleverly devised an algorithm to reduce a $(q + m)$ impulsive action sequence to the equivalent q-one, without any increase in the cost. The new q impulses occur at the same times and directions as those in the original $(q + m)$ sequence. Unfortunately, it only applies for l_2-optimization.

This impulse reduction algorithm is termed hereafter as *pruning*, as it effectively prunes redundant impulses from an initial, fuel-optimal candidate sequence, generated over a dense independent grid $\mathcal{T}$. This enables to disregard the design of the impulses execution times τ_i, eliminating it from the set of decision variables. For linear systems, the algorithm guarantees to achieve the solution of the optimization problem.

The method presented here follows Prussing's discussion on the topic.[31] Consider the fuel-optimal regulation problem

$$\begin{aligned}
\underset{\mathbf{U}_i}{\arg\min} \quad & J = \sum_i \|\mathbf{U}_i\|_2 \\
\text{subject to} \quad & \mathbf{s}_f - \Phi(t_f, t_0)\,\mathbf{s}_0 = \sum_i \Phi(t_f, t_i)\, B\, \mathbf{U}_i \,, \\
& \mathbf{s}(t_0) = \mathbf{s}_0 \,, \\
& \mathbf{s}(t_f) = \mathbf{0} \,.
\end{aligned}$$

At the k-th recursion, the candidate $(q + m - k)$ sequence $\mathbf{U}_i^k$ is updated through

$$\mathbf{U}_i^{k+1} = \frac{\mu_i}{\|\mathbf{U}_i^k\|_2}\mathbf{U}_i^k \,, \quad \forall i \,, \quad k = 0, 1, 2..., m \,, \tag{11}$$

where the weights μ_i are defined through

$$\beta_i = \frac{\alpha_i}{\|\mathbf{U}_i^k\|_2} \,, \quad \beta_r = \max \beta_i \,, \quad \mu_i = \|\mathbf{U}_i^k\|_2 \left(1 - \frac{\beta_i}{\beta_r}\right) . \tag{12}$$

DOI: 10.13009/EUCASS2023-057

The α-coefficients are defined as the linear coordinates spanning the kernel of the following application

$$\left(\hat{\mathbf{U}}_1 \quad \hat{\mathbf{U}}_2 \quad \dots \quad \hat{\mathbf{U}}_{q+m-k}\right)\boldsymbol{\alpha} = \mathbf{0}\,, \quad \hat{\mathbf{U}}_i = \frac{\mathbf{U}_i^k}{||\mathbf{U}_i^k||_2}\,. \tag{13}$$

which, for the k-th sequence, is an indeterminate linear system. The signs of α_i are globally selected to satisfy

$$\sum_i \alpha_i \geq 0\,. \tag{14}$$

Given an initial candidate sequence $\{\mathbf{U}\}$, this algorithm can be run m times to obtained the *pruned* sequence of q impulses.

5. Proximal Operators and Alternating Direction Method of Multipliers

The main technical novelty of this work is the complete application of Alternating Direction Method of Multipliers (ADMM) in its full potential as the main solver for the regulation problems of interest, given its ability to provide close-form, algorithmic solutions to general optimization problems. The use of ADMM as our main optimization solver will enable close-form solutions to general L_p-regulation problem, as detailed example by example in the following Section.

ADMM is an algorithm intended to blend the decomposability of dual ascent with the superior convergence properties of the method of multipliers, and is highly used as general convex optimization technique.[32] ADMM, as an operator splitting algorithm, takes the form of a decomposition-coordination procedure, in which the solutions to small local subproblems are coordinated to find a solution to the large global, original problem.

ADMM addresses the following consensus optimal problem,

$$\begin{aligned} \underset{\mathbf{x},\,\mathbf{z}}{\arg\min} \quad & f(\mathbf{x}) + g(\mathbf{z})\,, \\ \text{subject to} \quad & A\mathbf{x} - B\mathbf{z} = \mathbf{c}\,. \end{aligned} \tag{15}$$

The ADMM solution is first given by introducing the following Augmented Lagrangian to be minimized

$$L\left(\mathbf{x}, \mathbf{z}, \mathbf{u}\right) = f(\mathbf{x}) + g(\mathbf{z}) + (\rho/2)\,||A\mathbf{x} - B\mathbf{z} - \mathbf{c} + \mathbf{y}||_2^2 + D$$

where D is some additive constant, $\rho > 0$ is a penalty constant and $\mathbf{y}$ is the dual problem decision variable. The use of Augmented Lagrangian formalism is of relevance because it provides a much more robust algorithm than classical dual ascent, for example, converging even when f takes non-definite values or is strictly non-convex.[32]

Once introduced, the Lagrangian is minimized by the following iterates, providing the close-form solution to the original problem

$$\mathbf{x}^{k+1} = \arg\min_{\mathbf{x}} L_\rho\left(\mathbf{x},\, \mathbf{z}^k,\, \mathbf{y}^k\right)\,, \tag{16}$$

$$\mathbf{z}^{k+1} = \arg\min_{\mathbf{z}} L_\rho\left(\mathbf{x}^{k+1},\, \mathbf{z},\, \mathbf{y}^k\right)\,, \tag{17}$$

$$\mathbf{y}^{k+1} = \mathbf{y}^k + \rho\left(A\,\mathbf{x}^{k+1} - B\,\mathbf{z}^{k+1} - \mathbf{c}\right)\,. \tag{18}$$

The iterates need to be finished under appropriate terminating conditions, which are discussed in-depth in Boyd.[32]

Under the following two conditions: 1) f and g are closed, proper, and convex; their epigraphs are nonempty closed convex sets; 2) strong duality holds, the unaugmented Lagrangian has a saddle point; the ADMM iterates provide the following relevant convergence results:

1. Residual convergence. $A\,\mathbf{x}^k - B\,\mathbf{z}^k - \mathbf{c} = \mathbf{r}^k \to \mathbf{0}$ as $k \to \infty$; the iterates approach feasibility.

2. Objective convergence. $f(\mathbf{x}^k) + g(\mathbf{z}^k) \to J^+$ as $k \to \infty$, the objective function of the iterates approaches the optimal value.

Still, ADMM will be practically useful mostly in cases when modest accuracy is sufficient, even whenever one of the two assumptions do not hold. Moreover, ADMM will converge even when the minimization steps are not carried out exactly. This will be especially useful given the possibility of performing further pruning of candidate impulsive sequences, as in our case.

DOI: 10.13009/EUCASS2023-057

Moreover, the particular consensus equation $\mathbf{x} - \mathbf{z} = \mathbf{0}$ leads to the following $\mathbf{x}$-minimization

$$\mathbf{x}^{+} = \arg\min_{\mathbf{x}} \left(f(\mathbf{x}) + (\rho/2)\, \|\mathbf{x} - \mathbf{v}\|_2^2 \right) ,$$

where the righthand side is identified with a proximal operator,[33] denoted $\mathrm{prox}_{f,\rho}\mathbf{v}$. The $\mathbf{x}$-minimization in the proximity operator is generally referred to as proximal minimization. This work is highly founded on general, analytical or close-form proximal minimizations, as it will become apparent in the following sections.

The remaining free decision variables are the impulsive times τ_i at which the control sequence and the flow map are evaluated. The impulsive times define the independent grid $\mathcal{T} = \{\tau_i\}_{\forall i}$.

6. Naïve solution via dual-based Linear Programming

The motivation for this work is found in previous results by Le Cleac'h and Manchester,[10] which successfully demonstrated the use of the ADMM algorithm for space trajectory optimization, by consensing both an L_1 and L_2 fuel optimizations by means of a hybrid cost function. Their close-form solution is fundamentally constructed upon the discrete Linear Quadratic Regulator (LQR), while further simplification is possible if the problem is transcribed into its dual, Lagrange-multiplier/co-state form, as indicated in Barea et al.[34] Such solution is depicted here now as a preliminary step towards full exploitation of the ADMM scheme.

Consider the unconstrained l_1 fuel-optimal problem

$$\begin{aligned}
\arg\min_{\mathbf{U}_i} \quad & J = \sum_i \|\mathbf{U}_i\|_1 \\
\text{subject to} \quad & \mathbf{s}_f - \Phi(t_f, t_0)\, \mathbf{s}_0 = \sum_i \Phi(t_f, t_i)\, B\, \mathbf{U}_i \, , \\
& \mathbf{s}(t_0) = \mathbf{s}_0 \, , \\
& \mathbf{s}(t_f) = \mathbf{0} \, ,
\end{aligned} \tag{19}$$

to be solved via the ADMM technique. To achieve so, the following consensus, separable problem is introduced

$$\begin{aligned}
\arg\min_{\mathbf{x},\mathbf{z}} \quad & f(\mathbf{x}) + g(\mathbf{z}) \, , \\
\text{subject to} \quad & \mathbf{X} - \mathbf{Z} = \mathbf{0} \, , \\
& f(\mathbf{x}) = \alpha \sum_i \|\mathbf{x}_i\|_1 \, , \\
& g(\mathbf{z}) = \sum_i \mathbf{z}_i^\intercal \mathbf{z}_i + \mathcal{I}_C\,(\mathbf{Z}) \, , \\
& \mathbf{X} = \mathrm{ver}\{\mathbf{x}_i\}, \quad \mathbf{Z} = \mathrm{ver}\{\mathbf{z}_i\}, \qquad \forall i \, .
\end{aligned} \tag{20}$$

The indicator function $\mathcal{I}_C$ is defined for the flow map $C = \{\mathbf{Z} \in \mathrm{R}^{3N} \mid \hat{\Phi}\, \mathbf{Z} = \mathbf{s}_f - \Phi(t_f, t_0)\, \mathbf{s}_0\}$ as

$$\mathcal{I}_C = \begin{cases} 0 & \text{if} \quad \mathbf{Z} \in C \\ \infty & \text{if} \quad \mathbf{Z} \notin C \end{cases}$$

The resulting ADMM iterates are now described. First, the proximal minimization for $\mathbf{x}$ is given by a scalar soft-thresholding update[32]

$$x_i^{k+1} = \max\left(0,\, z_i^k - y_i^k - \alpha/\rho\right) - \max\left(0,\, -z_i^k + y_i^k - \alpha/\rho\right) .$$

For the $\mathbf{z}$-case, its minimization step is equivalent to the discrete LQR, as mentioned previously. However, exploiting Lagrange's formula and the indirect formulation of the minimization of $g(\mathbf{z})$ leads to a root-finding problem of reduced dimensionality for the Lagrange multiplier, solvable by means of Linear Programming techniques.

First, the corresponding unconstrained augmented Lagrangian is introduced

$$\begin{aligned}
J^{+} &= \sum_i^N \mathbf{z}_i^\intercal \mathbf{z}_i + \frac{\rho}{2}\,(\mathbf{z}_i - \mathbf{x}_i - \mathbf{y}_i)^\intercal\,(\mathbf{z}_i - \mathbf{x}_i - \mathbf{y}_i) + \lambda^\intercal \left(\mathbf{s}_d\,(t_f) - \Phi(t_f, t_0)\, \mathbf{s}\,(t_0) - \sum_{i=1}^N \Phi(t_f, t_i) B\, \mathbf{z}_i \right) = \\
&= \sum_i^N \mathbf{z}_i^\intercal \mathbf{z}_i + \frac{\rho}{2}\,(\mathbf{z}_i - \mathbf{x}_i - \mathbf{y}_i)^\intercal\,(\mathbf{z}_i - \mathbf{x}_i - \mathbf{y}_i) + \lambda^\intercal \left(\mathbf{e} - \sum_{i=1}^N \Phi(t_f, t_i)\, B\, \mathbf{z}_i \right)
\end{aligned}$$

DOI: 10.13009/EUCASS2023-057

The necessary conditions for optimality are given by the Lagrangian function's stationary point with respect to $(\mathbf{z}_i, \boldsymbol{\lambda})$, resulting in the following $3N + 6$ equations for the $3N + 6$ variables

$$\begin{aligned} \mathbf{z}_i + \rho\,(\mathbf{z}_i - \mathbf{x}_i - \mathbf{y}_i) - B^\intercal\,\Phi(t_f, t_i)^\intercal \boldsymbol{\lambda} = \mathbf{0}\ , \\ \mathbf{e} - \sum_{i=1}^{N} \Phi(t_f, t_i)\,B\,\mathbf{z}_i = \mathbf{0}\,. \end{aligned} \tag{21}$$

Solving for $\boldsymbol{\lambda}$ reads the following linear system

$$\left[\mathbf{e} - \frac{\rho}{1+\rho}\sum_i \Phi(t_f, t_i)\,B\,\left(\mathbf{x}_i + \mathbf{y}_i\right)\right] = \left[\sum_i B^\intercal\,\Phi(t_f, t_i)^\intercal\,\Phi(t_f, t_i)\,B\right]\boldsymbol{\lambda}\,, \tag{22}$$

where the controllability gramian maps the co-state to the natural dynamics error $\mathbf{e}$. It is interesting to note the feedforward role of the $\mathbf{x}$ vector of impulses. Once $\boldsymbol{\lambda}$ is obtained via efficient solving of the linear system, the L_2 impulses $\mathbf{z}_i$ are computed using the previous result, thus completing the ADMM iterates. Physically, this L_1-L_2 consensus solution represents the same energy sequence, which applies for different actuator configurations, for which the different either L_1 or L_2-norm is appropriate.

7. Optimal linear ADMM regulation

Building on the previous both theoretical and practical results, this Section presents the integral application of the ADMM close-form algorithm to the L_p fuel-optimal problem, in various of its common forms.

7.1 ADMM solution for l_2-optimization

The case for $p = 2$ will be first considered, for which both the pruner and classical PVT applies. The particularisation of this problem of interest is given again by

$$\begin{aligned} \underset{\mathbf{U}_i}{\arg\min} \quad & J = \sum_i \|\mathbf{U}_i\|_2 \\ \text{subject to} \quad & \mathbf{s}_f - \Phi(t_f, t_0)\,\mathbf{s}_0 = \sum_i \Phi(t_f, t_i)\,B\,\mathbf{U}_i\ , \\ & \mathbf{s}(t_0) = \mathbf{s}_0\ , \\ & \mathbf{s}(t_f) = \mathbf{0}\ , \\ & 0 \le \|\mathbf{U}_i\|_2 \le u_{\max}\,. \end{aligned} \tag{23}$$

Again, to exploit the ADMM algorithm, the separable form of the problem reads as follows

$$\begin{aligned} \underset{\mathbf{x},\,\mathbf{z}}{\arg\min} \quad & f(\mathbf{x}) + g(\mathbf{z})\,, \\ \text{subject to} \quad & \mathbf{x} - \mathbf{z} = \mathbf{0}\,, \\ & f(\mathbf{x}) = \mathcal{I}_C\,(\mathbf{X})\,, \\ & g(\mathbf{z}) = \sum_i \|\mathbf{z}_i\|_2 + \mathcal{I}_{\mathcal{B}}\,(\mathbf{z}_i)\,. \end{aligned} \tag{24}$$

In this case, f represents the indicator function of the flow map set $C = \{\mathbf{X} \in \mathrm{R}^{3N}\,|\,\hat{\Phi}\,\mathbf{X} = \mathbf{s}_f - \Phi(t_f, t_0)\,\mathbf{s}_0\}$. On the other hand, g both penalizes fuel consumption and constrains the impulses to lie on a ball of maximum radius $u_{\max}$ $\mathcal{B} = \{\mathbf{z} \in \mathbb{R}^3\,|\,0 \le \|\mathbf{z}_i\|_2 \le u_{\max}\}$.

The solution is given by the iteration of the following system of proximal minimizations

$$\mathbf{X}^{k+1} = \left(I - \hat{\Phi}^\dagger\hat{\Phi}\right)(\mathbf{Z}^k - \mathbf{Y}^k) + \hat{\Phi}^\dagger\left[\mathbf{s}_f - \Phi(t_f, t_0)\,\mathbf{s}_0\right]\,, \tag{25}$$

$$\mathbf{z}_i^{k+1} = \max\left(0, 1 - \frac{1}{\rho\,\|\mathbf{x}_i^{k+1} + \mathbf{y}_i^k\|}\right)\left(\mathbf{x}_i^{k+1} + \mathbf{y}_i^k\right)\,, \tag{26}$$

$$\mathbf{z}_i^{k+1} = \min\left(\|\mathbf{z}_i^{k+1}\|, u_{\max}\right)\mathbf{z}_i^{k+1} / \|\mathbf{z}_i^{k+1}\|\,, \tag{27}$$

$$\mathbf{Y}^{k+1} = \mathbf{Y}^k + \mathbf{X}^{k+1} - \mathbf{Z}^{k+1}\,. \tag{28}$$

DOI: 10.13009/EUCASS2023-057

The dagger operator in $\hat{\Phi}^{\dagger}$ indicates the Moore-Penrose pseudo-inverse and the use of the upper-case vectors $\mathbf{X}$, $\mathbf{Z}$ refers to vertical concatenation of the whole sequence. The first update is the projection of $\mathbf{X}$ on the convex set $A\mathbf{X} = \mathbf{b}$. The update of Z is performed block-wise and is the proximal operator of the l_2-norm (block soft-thresholding operator). Because all vector norms are convex and the set $\mathcal{B}$ is also convex, the algorithm shows dual convergence, and both primal and dual feasibility (in both $\mathbf{Z}^{k+1}$ and $\mathbf{X}^{k+1}$).

The asymmetric nature of the ADMM in the $\mathbf{X}$ and $\mathbf{Z}$ updates has physical implications in the resulting solution. At such, the resulting $\mathbf{X}$ sequence is flow-feasible, reading it is designed to achieve the regulation of the relative state (rendezvous the spacecraft). However, the final $\mathbf{Z}$ is hardware-feasible and fuel-optimal, but it may not result in total regulation. Because of the residual convergence properties of ADMM, this difference will end up being numerically negligible.

The final converged solution is in general non-sparse, but whose objective value is nearly optimal. As we have already introduced, for linear systems under impulsive control, a maximum number of q impulses exists, which is also optimal, and can be recovered from an initial guess. Thus, the converged primal sequence of impulses $\mathbf{X}$ is pruned to compute the optimal sequence, yielding an close-form optimal and sparse impulsive sequence.

The use of the indicator function and the set-oriented definition of the flow constraint allows to explicitly achieve close-form solutions without the need of continuation techniques of any ruling parameter α between the L_1/L_2 optimizations, compared to previous studies, like in Le Cleac'h.[10]

7.2 ADMM dual-based solution for l_2-optimization

A more advanced form of the previous solution directly addresses the optimality conditions given by Carter's PVT solution, yielding a formulation of the l_2-problem in its dual variables or co-states.

Solving Carter's problem has been proven to be non-polynomial and non-convex, in general requiring of advanced numerical machinery to be properly solved.[7] However, the combination of the ADMM with the pruning algorithm can be shown to provide optimal results at nearly null computational expenses. Moreover, despite the loss of the convergence conditions for the ADMM solution, the algorithm is still capable of providing solutions which satisfy the necessary and sufficient conditions of optimality almost to numerical precision.

Defining the following partitions of the decision vectors $\mathbf{X}$, $\mathbf{Z}$ and $\mathbf{Y}$

$$\mathbf{X} = \begin{pmatrix} \mathbf{X}_v & \mathbf{X}_p \end{pmatrix}^{\intercal}, \quad \mathbf{Z} = \begin{pmatrix} \mathbf{Z}_v & \mathbf{Z}_p \end{pmatrix}^{\intercal}, \quad \mathbf{Y} = \begin{pmatrix} \mathbf{Y}_v & \mathbf{Y}_p \end{pmatrix}^{\intercal},$$

the problem, in a mixed direct-dual statement for the co-states and the associated impulses, is the following

$$\begin{aligned} \underset{\mathbf{p},\,\mathbf{U}}{\arg\min} \quad & J = \sum_i \Delta v_i \\ \text{subject to} \quad & \mathbf{s}_f - \Phi(t_f, t_0)\,\mathbf{s}_0 = \sum_i \Phi(t_f, t_i)\,B(t_i)\,\mathbf{U}_i\,, \\ & \mathbf{s}_f - \Phi(t_f, t_0)\,\mathbf{s}_0 = -\sum_i \Phi(t_f, t_i)\,B(t_i)\,\Delta v_i\,\mathbf{p}_i\,, \\ & \mathbf{s}(t_0) = \mathbf{s}_0\,, \\ & \mathbf{s}(t_f) = \mathbf{0}\,, \\ & \Delta v_i = ||\mathbf{U}_i||_2\,, \\ & 0 \le ||\mathbf{p}_i||_2 \le 1\,, \\ & \mathbf{p}_i = \mathbf{U}_i/||\mathbf{U}_i||\,. \end{aligned} \tag{29}$$

The flow map constraint appears both in its dual and direct statement to provide a symmetric update of the primer vector sequence in both the $\mathbf{X}$ and $\mathbf{Z}$ proximal minimizations. As such, a close-form solution of the problem is given by the following iterates

$$\mathbf{X}_v^{k+1} = \left(I - \hat{\Phi}^{\dagger}\hat{\Phi}\right)(\mathbf{Z}_v^k - \mathbf{Y}_v^k) + \hat{\Phi}^{\dagger}\left[\mathbf{s}_f - \Phi(t_f, t_0)\,\mathbf{s}_0\right], \tag{30}$$

$$\mathbf{x}_{p,i}^{k+1} = \mathbf{x}_{v,i}^{k+1} / ||\mathbf{x}_{v,i}^{k+1}||_2 \quad \text{if} \quad ||\mathbf{x}_{v,i}^{k+1}||_2 > 1\,, \tag{31}$$

$$\mathbf{z}_{v,i}^{k+1} = \max\left(0, 1 - \frac{1}{\rho\,||\mathbf{x}_{v,i}^{k+1} + \mathbf{y}_{v,i}^k||}\right)\left(\mathbf{x}_{v,i}^{k+1} + \mathbf{y}_{v,i}^k\right), \tag{32}$$

$$\mathbf{Z}_p^{k+1} = \left(I - \bar{\Phi}^{\dagger}\bar{\Phi}\right)(\mathbf{X}_p^{k+1} + \mathbf{Y}_p^k) + \bar{\Phi}^{\dagger}\left[\mathbf{s}_f - \Phi(t_f, t_0)\,\mathbf{s}_0\right], \tag{33}$$

$$\mathbf{Y}^{k+1} = \mathbf{Y}^k + \mathbf{X}^{k+1} - \mathbf{Z}^{k+1}\,. \tag{34}$$

DOI: 10.13009/EUCASS2023-057

The linear operator $\bar{\Phi}$ differs from its direct counterpart $\hat{\Phi}$ by definition

$$\bar{\Phi} = \mathrm{hor}\,\{-\Delta v_i\,\Phi(t_f, t_0)\Phi(t_i, t_0)^{-1}\}\,, \quad \hat{\Phi} = \mathrm{hor}\,\{\Phi(t_f, t_0)\Phi(t_i, t_0)^{-1}\}\,, \quad \forall i.$$

The $\mathbf{Z}_p$ update is actually non-linear, although the consensus form of the ADMM optimizations allows to treat it as a projection on a linear polyhedra set.

7.3 ADMM solution for l_1-optimization

The fuel-optimal case for $p = 1$ will be now studied. The l_1-problem is usually more difficult to solve than the l_2 one, given the lack of differentiability of the cost function.[13] However, under the ADMM paradigm, the solution is straigthforward.

The particularisation of this problem of interest is given again by

$$\begin{aligned} \underset{\mathbf{U}_i}{\arg\min} \quad & \text{Eqs. (19)} \\ \text{subject to} \quad & 0 \leq ||\mathbf{U}_i||_1 \leq u_{\max}\,. \end{aligned} \tag{35}$$

Again, the ADMM, separable form of the problem reads as follows

$$\begin{aligned} \underset{\mathbf{x},\mathbf{z}}{\arg\min} \quad & f(\mathbf{x}) + g(\mathbf{z})\,, \\ \text{subject to} \quad & \mathbf{x} - \mathbf{z} = \mathbf{0}\,, \\ & f(\mathbf{x}) = \mathcal{I}_C\,, \\ & g(\mathbf{z}) = \sum_i ||\mathbf{z}_i||_1 + \mathcal{I}_{\mathcal{B}}\,(\mathbf{z}_i)\,. \end{aligned} \tag{36}$$

The solution is trivially given by the iteration of the following system of proximal minimizations

$$\mathbf{X}^{k+1} = \left(I - \hat{\Phi}^{\dagger}\hat{\Phi}\right)(\mathbf{Z}^k - \mathbf{Y}^k) + \hat{\Phi}^{\dagger}\left[\mathbf{s}_f - \Phi(t_f, t_0)\,\mathbf{s}_0\right]\,, \tag{37}$$

$$z_i^{k+1} = \max\left(0,\, x_i^{k+1} + y_i^k - 1/\rho\right) - \max\left(0,\, -x_i^{k+1} - y_i^k - 1/\rho\right)\,, \tag{38}$$

$$z_i^{k+1} = \max\left(0,\, z_i^{k+1} - \lambda\right) - \max\left(0,\, -z_i^{k+1} - \lambda\right)\,, \tag{39}$$

$$\mathbf{Y}^{k+1} = \mathbf{Y}^k + \mathbf{X}^{k+1} - \mathbf{Z}^{k+1}\,. \tag{40}$$

The soft-thresholding $(\cdot)_+$ in the proximal minimization of the l_1-norm is performed entry-wise, via a scalar update, for each component of each impulse $\mathbf{z}_i^k$. The projection onto the ball $\mathcal{B}$ is achieved through the l_∞-norm, as stated by the Moreau decomposition (given they are dual operators[32]), which defines the λ parameter as

$$\lambda = \begin{cases} 0 & \text{if} \quad ||\mathbf{z}_i||_1 \leq z_{\max} \\ \underset{\lambda}{\arg\min} \sum_j^3 \left(|z_{i,j}| - \lambda\right)_+ = z_{\max} & \text{if} \quad ||\mathbf{z}_i||_1 > z_{\max} \end{cases}$$

l_1-optimal impulsive sequences are also used to promote sparsity, yielding actions plans of low control frequency, which are desirable from both an operational and hardware perspective. It is natural to couple the presented optimization with the intersection of the $\mathcal{B}$-ball with the cardinality set $\mathcal{D} = \{\mathbf{Z}\,|\,\mathrm{card}(\mathbf{Z}) \leq n\}$, so that the final ADMM problem is modified to

$$g(\mathbf{z}) = \sum_i ||\mathbf{z}_i||_1 + \mathcal{I}_{\mathcal{B}\bigcup\mathcal{D}}(\mathbf{z}_i)\,. \tag{41}$$

After the re-definition of the indicator function $\mathcal{I}_{\mathcal{B}}$, the close-form solution for the $\mathbf{z}$ proximal minimization is analytically adapted to

$$z_i^{k+1} = \max\left(0, x_i^{k+1} + y_i^k - 1/\rho\right) - \max\left(0, -x_i^{k+1} - y_i^k - 1/\rho\right)\,,$$

$$z_i^{k+1} = \max\left(0,\, z_i^{k+1} - \lambda\right) - \max\left(0,\, -z_i^{k+1} - \lambda\right)\,,$$

$$\mathbf{z}_i = \begin{cases} \mathbf{0} & \text{if} \quad ||\mathbf{z}_i||_1 \notin \mathcal{D}_s \\ \mathbf{z}_i & \text{if} \quad ||\mathbf{z}_i||_1 \in \mathcal{D}_s \end{cases}\,,$$

which results in keeping the n larger impulses and nullyfing the rest. This example shows how the ADMM algorithm can render trivial solutions to highly complex control optimization problems, at low computational cost.

DOI: 10.13009/EUCASS2023-057

8. Optimal nonlinear ADMM regulation

The presented guidance, trajectory planning techniques presented benefit from surrogate relative motion models when addressing the regulation problem at hands, mainly based on an appropriate linearization of true nonlinear dynamics and the corresponding STM $\Phi(t, t_0)$. Therefore, any control policy $\mathbf{\Pi}(t)$ computed under such dynamics is not guaranteed to regulate the relative state vector under the true nonlinear field. In general, some form of feedback is needed to successively refined $\mathbf{\Pi}(t)$ and $\phi(t, t_0)$ to comply with the nonlinear relative motion dynamics. This is achieved through iterating a backward-forward pass or sweep structure until convergence, which may be implemented online through Model Predictive Control (MPC), as described now.

MPC is an optimal control technique based on iterative optimization, introduced in the late 1980s,[35,36] which shows a long tradition within rendezvous and proximity operations studies.[21,37–42] In the MPC paradigm, an optimal surrogate guidance problem is solved for a given time horizon $t_i = 0, 1, ..., T$; and as a result, both a state trajectory $\{\mathbf{s}_i(t_i)\} = \mathbf{s}_1, \mathbf{s}_2, ..., \mathbf{s}_T$ and control action policy $\{\mathbf{U}_i(t_i)\} = \mathbf{U}_1, \mathbf{U}_2, ..., \mathbf{U}_T$ are returned. The controller only executes the action at the initial time $\mathbf{U}_1$, and, after the plant natural rollout one time step ahead, the optimization problem is run again with the time horizon receded $t_i = 0, 1, ..., T-1$. In this way, the true nonlinearities and unmodelled uncertainties in the surrogate guidance model are accommodated through a time-receding horizon scheme under the true plant dynamics.

9. Applications and mission cases

9.1 Hill-Clohessy-Wiltshire Keplerian rendezvous

The first mission design scenario applies for a HCW rendezvous scenario, in which the traslational relative state between the target and chaser spacecraft is to be regulated, as given in Section 2.

It is customary to use canonical units, so that $\mu = 1$ for the given reference orbit semimajor axis r_t. The mission time of flight is selected to be $t_f = 2\pi$ (one orbital period).

Following Alfriend et al.,[43] the initial relative conditions are given by

$$\mathbf{s}_0 = \begin{bmatrix} -0.005019 & 0.01 & 0.01 & 0.01 & 0.01 & 0 \end{bmatrix}^{\mathsf{T}},$$

which corresponds to bounded, librating relative motion.

The mission time is discretized into equally spaced 500 grid points, in which an impulse may or may not occur.

Initially, the unconstrained l_2-norm fuel optimal problem is considered. After resolving the 500 impulses, sparsity in the initial candidate sequence is promoted through the PVT pruner, which is used to refine the sequence and reduce it down to 6 maneuvers only. Figs. 1 depicts the converge results, while Fig. 3 demonstrates that the sequence is effectively able to rendezvous the two spacecraft (strict regulation of the final relative state).

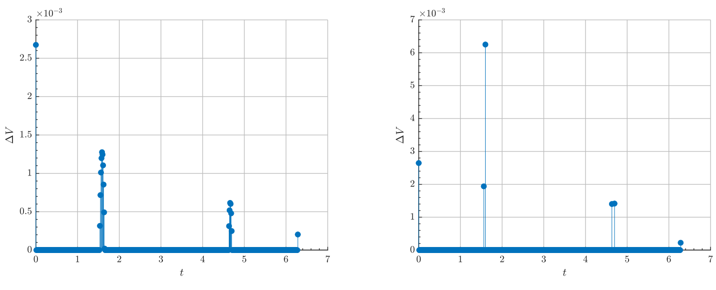

(a) Candidate ADMM solution. (b) Pruned PVT solution.

Figure 1: Final candidate and pruned impulse sequences for the direct formulation of the l_2-problem.

The same problem is solved via the dual formulation of the l_2-ADMM solution, in which the primer vector optimality conditions are directly addressed. Again, Figs. 2 shows the final sequence solutions, while the regulation of the relative state is depicted again in Fig. 3. Note how the candidate solution is already composed of 6 impulses only, satisfying the optimality conditions of the problem. Comparison between the direct and indirect formulation is addressed in Fig. 4, in which the convergence of both algorithms towards the fundamental PVT cost limit is graphically demonstrated.

DOI: 10.13009/EUCASS2023-057

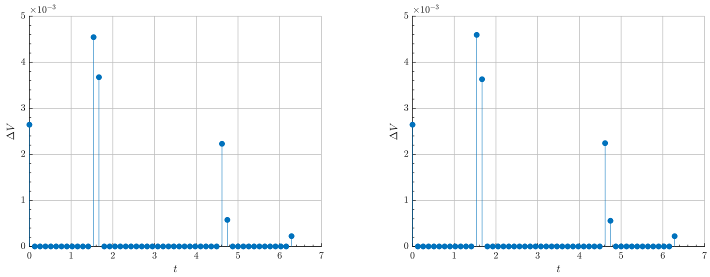

(a) Candidate ADMM solution. (b) Pruned PVT solution.

Figure 2: Final candidate and pruned impulse sequences for the indirect formulation of the l_2-problem.

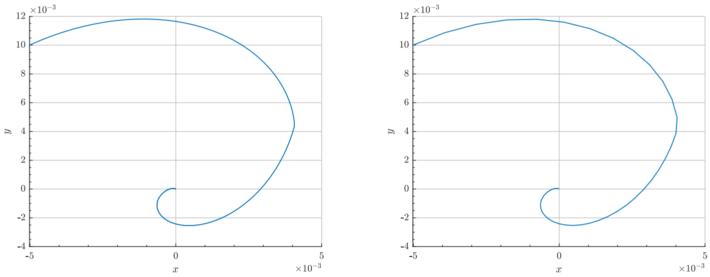

(a) Direct solution. (b) Indirect solution.

Figure 3: Regulation of the relative state in the l_2-problem.

Finally, similar results are also presented for the l_1-problem, which is additionally constrained to respect a maximum control authority of $\Delta V = 0.001$ and achieve the rendezvous in less than 20 impulses, via a cardinality constraint. Despite the additional complexity, the algorithm still solves the problem at null computational burden. Its results can be analysed in Figs. 5a and 5b.

Table 2 summarizes the main performance metrics of the three algorithms proposed.

Table 2: Main performance indices for Scenario I.

	l_2-ADMM	**l_2-dual ADMM**	**l_1-ADMM**
Sequence cost	0.0139	0.0139	0.0184
ADMM/PVT cost ratio	0.9932	0.9993	N/A
Computational time [s]	1.64	1.36	4.54
Final state error	4.4043×10^{-16}	5.3436×10^{-16}	8.1811×10^{-16}

9.2 Impulsive cislunar rendezvous

The MPC-ADMM naïve solution to the l_1-fuel optimal problem is applied for a practical case of orbital rendezvous between two northern halo orbits in the Earth-Moon L_2 Lagrange point.

The initial conditions of both the target spacecraft $\mathbf{S}_t$ and the relative state $\boldsymbol{s}$ in the normalized, synodic frame are given by

$$\mathbf{S}_t = \begin{bmatrix} 1.1049 & 0.0216 & -0.0431 & 0.0035 & 0.2138 & 0.0298 \end{bmatrix},$$
$$\boldsymbol{s} = \begin{bmatrix} 0.0126 & -0.0216 & 0.0235 & -0.0035 & -0.0296 & -0.0298 \end{bmatrix}.$$

The mission time of flight is selected to be $t_f = \pi$ (14 days). The rendezvous mission shall be accomplished via 40 impulses. The final results, in terms of the impulsive sequence and the final state evolution, may be found in Fig. 6, in which the regulation of the relative state can be appreciated.

DOI: 10.13009/EUCASS2023-057

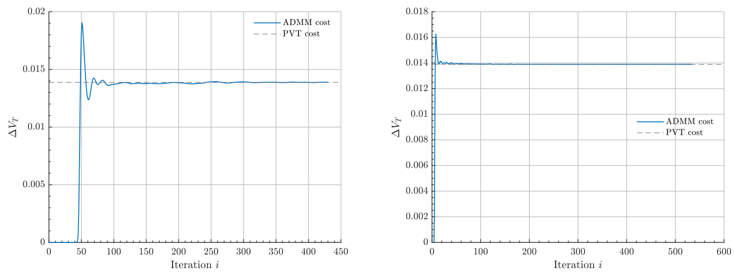

(a) Convergence ratio of the direct solution.

(b) Convergence ratio of the indirect solution.

Figure 4: Comparison between the l_2-problem direct and indirect solutions in terms of control effort.

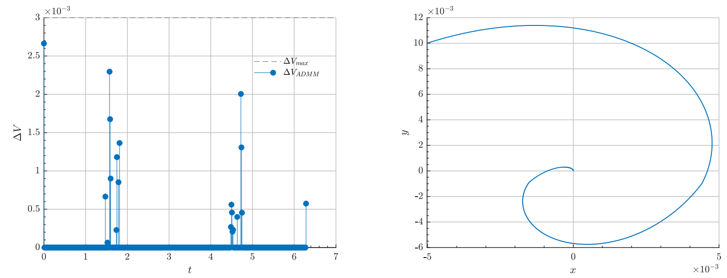

(a) Final impulse sequences for the l_1-problem.

(b) Regulation of the relative state for the l_1-problem.

Figure 5: Final impulse sequence and relative state regulation of the l_1-problem.

9.3 Boresight pointing

The presented algorithms can be easily adapted to optimal attitude planning. In this case, successive linearization together with an MPC scheme are used to optimally plan the needed torque law to achieve the following rest-to-rest slew, characterized by final and initial conditions

$$\mathbf{s}_0 = \begin{bmatrix} 0 & 0 & 0 & 1 & 0 & 0 & 0 \end{bmatrix}^\intercal , \quad \mathbf{s}_f = \begin{bmatrix} 0 & 0 & \sin(\pi/8) & \cos(\pi/8) & 0 & 0 & 0 \end{bmatrix}^\intercal ,$$

which corresponds to a rotation of 45° around the body z-axis, to be performed via equally spaced 100 maneuvers in up to 600 seconds. The algorithm successfully achieves the regulation of the relative state, resulting in the desired slew, as shown in Fig. 7.

10. Conclusions

This work proposes novel formulations of constrained, time-fixed, linear and nonlinear fuel-optimal impulsive control problems in astrodynamics, in the form of general consensus optimization. A novel combination of Proximal Operators and classical Primer Vector Theory is presented, yielding a really low footprint, accurate and fast optimal control solver. Comparing its performance and capacities to standard convex optimization techniques, the proposed solver stands as a solid candidate for real-time, embedded guidance applications.

In particular, candidate L_p-norm fuel-optimal control sequences are generated through Alternating Direction Method of Multipliers. The feasible sequence is then pruned and refined through classical Primer Vector Theory results, promoting sparsity and further reduction of the cost function, if necessary. For the q-dimensional linear case, the pruned sequence of q-impulses is shown to be optimal. The methodology is further extended for nonlinear systems in combination with Model Predictive Control. In addition, ADMM is also used to close the gap between L_1 and L_2 optimization in classical astrodynamics problems, allowing to establish a cost mapping principle between fuel-optimal and quadratic-cost problems; second, this latter L_2 optimization is solved exploiting its dual-problem multi-stage formulation, for which a close-form solution exists. All in all, the combination of these two techniques allows to render general NLP fuel-optimal problems solvable by Linear Programming techniques.

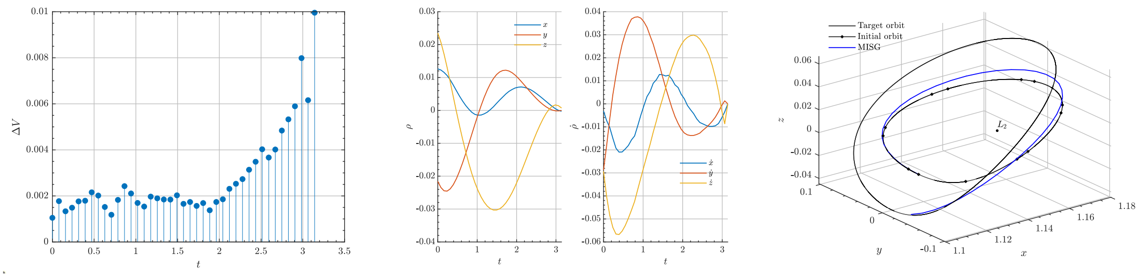

(a) MPC-ADMM control sequence. (b) Regulation of the relative state. (c) Synodic rendezvous trajectory.

Figure 6: Main performance results for Scenario II.

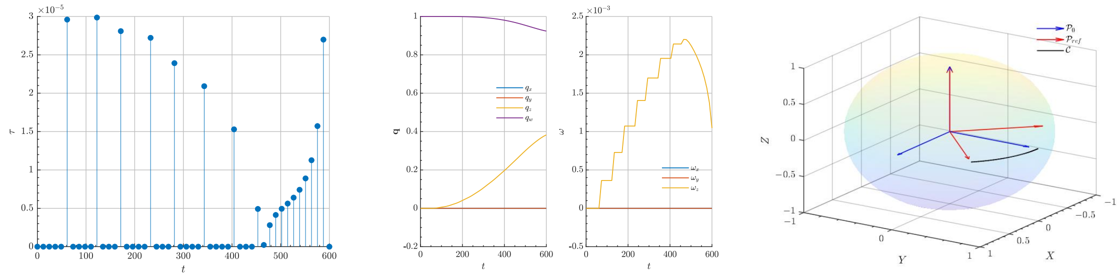

(a) MPC-ADMM torque sequence. (b) Regulation of the relative attitude. (c) Trajectory on the attitude sphere.

Figure 7: Main performance results for Scenario III.

11. Acknowledgments

S.C.d.V., H.U. and P.S.-L. wish to acknowledge the Spanish State Research Agency for their support through the research grants PID2020-112576GB-C22 funded by MCIN/AEI/ 10.13039/501100011033, and TED2021-132099B-C32 funded by MCIN/AEI/ 10.13039/501100011033 and by the “European Union NextGenerationEU/PRTR”.

References

[1] I.M. Ross and M. Karpenko. A review of pseudospectral optimal control: From theory to flight. *Annual Reviews in Control*, 36(2):182–197, 2012.

[2] T.N. Edelbaum. How many impulses? *Astronautics and Aeronautics*, pages 64–69, 1967.

[3] D.F. Lawden. Optimal trajectories for space navigation. *Butterworths*, 1963.

[4] L.W Neustadt. Optimization, a moment problem, and nonlinear programming. *Journal of The Society for Industrial and Applied Mathematics, Series A: Control*, 2:33–53, 1964.

[5] R.G. Stern and J.E. Potter. *Optimization of Midcourse Velocity Corrections*, pages 70–83. 1966.

[6] J.E. Prussing. *Optimal multi-impulse orbital rendezvous*. PhD thesis, Massachusetts Institute of Technology, 1967.

[7] D. Arzelier, C. Louembet, A. Rondepierre, and M. Kara-Zaitri. A new mixed iterative algorithm to solve the fuel-optimal linear impulsive rendezvous problem. *Journal of Optimization Theory and Applications*, 159, 10 2013.

[8] E. Taheri and J.L. Junkins. How many impulses redux. *The Journal of the Astronautical Sciences*, 67:257–334, 2020.

[9] D. Malyuta, Y. Yu, P. Elango, and B. Açïkmeçe. Advances in trajectory optimization for space vehicle control. *Annual Reviews in Control*, 52:282–315, 2021.

DOI: 10.13009/EUCASS2023-057

[10] S. Le Cleac'h and Z. Manchester. Fast solution of optimal control problems with l1 cost. In *Proceedings of AAS/AIAA Astrodynamics Specialist Conference*, 2019.

[11] K. Tracy and Z. Manchester. Model-predictive attitude control for flexible spacecraft during thruster firings. In *Proceedings of the AAS-AIAA Astrodynamics Specialist Conference*, 2020.

[12] L. Persson. *Model Predictive Control for Cooperative Rendezvous of Autonomous Unmanned Vehicles*. PhD thesis, KTH Royal Institute of Technology, 2021.

[13] I.M. Ross. Space trajectory optimization and l1-optimal control problems. In P. Gurfil, editor, *Modern Astrodynamics*, volume 1 of *Elsevier Astrodynamics Series*, pages 155–VIII. Butterworth-Heinemann, 2006.

[14] G.W. Hill. Researches in the lunar theory. *American Journal of Mathematics*, 1878.

[15] W. H. Clohessy and R. S. Wiltshire. Terminal guidance system for satellite rendezvous. *Journal of the Aerospace Sciences*, 27(9):653–658, 1960.

[16] J. Tschauner and P. Hempel. Optimale beschleunigeungsprogramme fur das rendezvous-manover. *Astronautica Acta*, 1964.

[17] R. G. Melton. Time-explicit representation of relative motion between elliptical orbits. *Journal of Guidance, Control, and Dynamics*, 23(4):604–610, 2000.

[18] A.I. Nazarenko. *State transition matrix of relative motion for the non-circular orbit. Relation with partial-derivative matrix in the satellite coordinate system.*

[19] T. E. Carter. State transition matrices for terminal rendezvous studies: Brief survey and new example. *Journal of Guidance, Control, and Dynamics*, 21(1):148–155, 1998.

[20] K. Yamanaka and F. Ankersen. New state transition matrix for relative motion on an arbitrary elliptical orbit. *Journal of Guidance, Control, and Dynamics*, 25(1):60–66, 2002.

[21] S. Cuevas del Valle, H. Urrutxua, P. Solano-López, R. Gutierrez-Ramon, and A. K. Sugihara. Relative dynamics and modern control strategies for rendezvous in libration point orbits. *Aerospace*, 9(12), 2022.

[22] S. Cuevas del Valle, H. Urrutxua, and P. Solano-López. Optimal floquet stationkeeping under the relative dynamics of the three-body problem. *Aerospace*, 10(5), 2023.

[23] R. J. Luquette. *Nonlinear control design techniques for precision formation flying at Lagrange points*. PhD thesis, University of Maryland, 2006.

[24] David L. Richardson. A note on lagrangian formulations for motion about the collinear points. *Celestial Mechanics*, 22:231–236, 1980.

[25] J. Solá. Quaternion kinematics for the error-state kalman filter, 2017.

[26] P. M. Lion and M. Handelsman. Primer vector on fixed-time impulsive trajectories. *AIAA Journal*, 6(1):127–132, 1968.

[27] D. Jezewski. Primer vector theory applied to the linear relative-motion equations. *Optimal Control Applications and Methods*, 1(4):387–401, 1980.

[28] J.E. Prussing. *Primer Vector Theory and Applications*, pages 16–36. 2010.

[29] T. E. Carter. Necessary and sufficient conditions for optimal impulsive rendezvous with linear equations of motion. *Dynamics and Control*, 10(1):219–227, 2000.

[30] L. W. Neustadt. A general theory of minimum-fuel space trajectories. *Journal of the Society for Industrial and Applied Mathematics Series A Control*, 3(2):317–356, 1965.

[31] J.E. Prussing. Optimal impulsive linear systems: Sufficient conditions and maximum number of impulses. *The Journal of the Astronautical Sciences*, 43:195–206, 1995.

[32] S. Boyd, E. Parikh, N.Chu, B. Peleato, and J. Eckstein. *Distributed Optimization and Statistical Learning via the Alternating Direction Method of Multipliers*. Standford University, 2010.

DOI: 10.13009/EUCASS2023-057

[33] N Parikh and S. Boyd. *Proximal Algorithms*. Standford University, 2013.

[34] A Barea, H. Urrutxua, and L. Cadarso. Dual-based method for global optimization of impulsive orbital maneuvers. *The Journal of the Astronautical Sciences*, 69:1666–1690, 2022.

[35] E.F. Camacho and C. Bordons. *Model Predictive Control*. Springer, 1998.

[36] M. Schwenzer, M. Ay, T. Bergs, and D. Abel. Review on model predictive control: an engineering perspective. *The International Journal of Advanced Manufacturing Technology*, 117:1327–1349, 2021.

[37] A. Richards and J. How. Performance evaluation of rendezvous using model predictive control. *AIAA Guidance, Navigation, and Control Conference and Exhibit*, 11 2003.

[38] L. Breger and J. How. J2-modified gve-based mpc for formation flying spacecraft. 08 2012.

[39] F. Gavilan, R. Vazquez, and E. F. Camacho. Chance-constrained model predictive control for spacecraft rendezvous with disturbance estimation. *Control Engineering Practice*, 20(2):111–122, 2012.

[40] E. N. Hartley. A tutorial on model predictive control for spacecraft rendezvous. In *2015 European Control Conference (ECC)*, pages 1355–1361, 2015.

[41] A. Richards and J. How. Analytical performance prediction for robust constrained model predictive control. *International Journal of Control*, 79, 08 2006.

[42] J. Sánchez, F. Gavilán, and R. Vázquez. Chance-constrained model predictive control for near rectilinear halo orbit spacecraft rendezvous. *Aerospace Science and Technology*, 100:105827, 03 2020.

[43] K.T. Alfriend, S.R Vadali, P. Gurfil, J.P. How, and L.S. Breguer. *Spacecraft Formation Flying: Dynamics, control and navigation*. Elsevier, 2010.